



**HAL**  
open science

# Feature extraction in palmprint recognition using spiral of moment skewness and kurtosis algorithm

Bilal Attallah, Amina Serir, Youssef Chahir

## ► To cite this version:

Bilal Attallah, Amina Serir, Youssef Chahir. Feature extraction in palmprint recognition using spiral of moment skewness and kurtosis algorithm. *Pattern Analysis and Applications*, 2019, 22 (3), pp.1197–1205. 10.1007/s10044-018-0712-5 . hal-01790989

**HAL Id: hal-01790989**

**<https://hal.science/hal-01790989>**

Submitted on 18 Sep 2018

**HAL** is a multi-disciplinary open access archive for the deposit and dissemination of scientific research documents, whether they are published or not. The documents may come from teaching and research institutions in France or abroad, or from public or private research centers.

L'archive ouverte pluridisciplinaire **HAL**, est destinée au dépôt et à la diffusion de documents scientifiques de niveau recherche, publiés ou non, émanant des établissements d'enseignement et de recherche français ou étrangers, des laboratoires publics ou privés.

# Feature extraction in palmprint recognition using spiral of moment skewness and kurtosis algorithm

Bilal Attallah<sup>1,2</sup> · Amina Serir<sup>1</sup> · Youssef Chahir<sup>2</sup>

## Abstract

Because of their high recognition rates, coding-based approaches that use multispectral palmprint images have become one of the most popular palmprint recognition methods. This paper describes a new multispectral palmprint recognition method that aims to further improve the performance of coding-based approaches by focusing on the local binary pattern (LBP) filters and spiral moments features. The final feature map is derived through a staged process of creating a composite of spiral and LBP features by fusing them together and passing the features through the minimum redundancy maximum relevance transformers. Using Hamming distances, the inter- and intra-similarities of the palmprint feature maps are determined. The experimental technique was evaluated using the available data on the IITD, MSPolyU and PolyU PPDB databases. The results indicate that the method achieved high levels of accuracy in the identification and verification modes. Furthermore, this method outperforms the existing advanced techniques.

**Keywords** Palmprint recognition · Spiral features · BSIF · mRMR · Hamming distance

## 1 Introduction

As security threats become increasingly sophisticated, the demand for biometric capability has increased. Services that demand authentication and high levels of data protection are increasingly reliant upon convenient biometric security. The scope for applying biometric security to identify and verify an individual through their physical or behavioral attributes [1] is broad. Forensic science and access control are two capacities that have stimulated an increase in biometric research. Several physical characteristics have been used for identification and verification purposes: face, fingerprint, gait, iris, keystroke and palmprint. Some of these characteristics are well established and widely implemented

in particular fields. Palmprint images are unique, reliable and stable; the techniques to distinguish palmprints are flexible, non-intrusive and user-friendly and have good discrimination capability. The principle lines, minutiae points, ridges, wrinkles and texture of palmprints are the features that confer their uniqueness.

Over the past 10 years, palmprint recognition has been the subject of investigation; this paper aims to contribute to the research by describing a new technique that further enhances the recognition accuracy by generating superior discrimination information during feature extraction. Among numerous emerging palmprint recognition techniques, the high recognition rates generated by coding-based methods of multispectral palmprint images are the most popular. Here, a new palmprint recognition method that fuses palm features is proposed to supersede the performance of the existing techniques.

At each of the three stages of the standard biometric cognition process, the experimental method is applied to promote recognition performance. The stages are (1) deriving the final feature code from the fusion of local binary patterns (LBP) and spiral moments features, (2) selecting the best features as determined using the minimum redundancy maximum relevance (mRMR) transformers and (3) matching using Hamming distance metric, which determines

---

✉ Bilal Attallah  
bilal.attallah@unicaen.fr

Amina Serir  
aserir@usthb.dz

Youssef Chahir  
youssef.chahir@unicaen.fr

<sup>1</sup> LTIR Laboratory, Electronic Department, USTHB, Algiers, Algeria

<sup>2</sup> UNICAEN, ENSICAEN, CNRS, GREYC, Normandie University, 14000 Caen, France

---

the inter- and intra-spectral similarities in palmprint feature maps. We tested the method with the IITD, MSPolyU and PolyU PPDB databases and show that the method has a high identification and verification accuracy: its identification rate is 99.57%, and its equal error rate (EER) is 0.0026. These results are superior to those of similar methods, e.g., in [2], the EER for the MSPolyU database is 0.0035 higher than our experimental method, and the methods in [3] have lower performance than the experimental method.

## 2 Related work

A key stage common to palmprint recognition systems is the feature extraction process. The goal of this step is to capture the most distinctive information from the region of interest (ROI) that has been identified. There are several algorithms for this purpose: structural-based approaches such as the local line direction patterns, Sobel/Canny edge lines or minutiae determined by the scale-invariant feature transform (SIFT) or Speeded Up Robust Features (SURF) [4]; appearance-based approaches, e.g., sub-space based on the EigenPalm and principal component analysis (PCA) [5]; statistical approaches such as Gabor and wavelet [2, 5]; coding-based methods (e.g., palm-code) [6]; and hybrid techniques such as 2D FLPP [7, 8].

Attracted by the success of coding-based methods that encode the responses of a bank of filters into bit-wise features, our interests lie with multiscale schemes that represent palm lines at higher scales. This approach has stimulated several algorithms. Based on a normalized 2D Gabor filter, Zhang et al. devised an effective palm-code algorithm [6]. Zuo et al. [9] and Kong et al. [5] used competitive coding to devise the multiscale-orientated 2D log-Gabor filters and encode the dominant orientation, respectively. Jia et al. [3] used the line orientation code founded on a modified finite Radon transform, which is similar to the competitive code. Zhang et al. [5] described a multispectral approach, where the features are extracted by competitive coding using six oriented 2D Gabor filters for each spectral band; a score fusion at the recognition stage completes the process. Gabor filters were also used by Tahmasebi et al. [5] to create a RankLevel fusion for a multispectral palmprint system. In [10], a different approach fused the features extracted by Gabor and matched the filters from the palmprint and vein palm to create a combined palmprint and palmvein verification system. Zuo et al. [11] used a sparse competitive code based on the second derivative of Gaussians with a bank of eighteen multiscale-oriented filters. The hierarchical approach of Hong et al. [12] fused a rough feature extraction using a block-dominant orientation code; this method was subsequently refined using a block-based histogram

of oriented gradients from different spectral bands. Cui et al. used a bidirectional representation derived from pattern classification [13]. Zhang et al. [14] collected recent advanced research works on multispectral biometrics including multispectral palmprint recognition. Xu et al. introduced a new multispectral palmprint recognition system based on the combination of a digital Shearlet transform and a multiclass projection extreme learning machine [15]. Fei et al. [7] described their method that used a double half-orientation bank of half-Gabor filters, which is defined for the half-orientation extraction. A double-orientation code based on Gabor filters and a nonlinear matching scheme is described in [8]. The methods in [7, 8] have been evaluated using the multispectral polytechnique palmprint database (MSPolyU).

The technique of competitive coding, which has been favored by some researchers, captures the discriminative-orientation information of the palm line contrast in a filtering process that uses the neurophysiology-based Gabor function. It has the competitive winner-takes-all rule. Inspired by the human visual system [16], this popular state-of-the-art, texture-based, feature extraction algorithm compares images of palm lines. Palm lines are specific multiscale features; in contrast to fine lines and wrinkles that are vulnerable to change or disappear depending on the lighting, the principal lines are well defined and clear at large scales. Palm lines are determined to be positive if they are bright and negative if they are dark [17].

In the spatial domain, a 2D Gabor function is a Gaussian multiplied by a complex exponential and can be considered a Gaussian shifted from the origin in the Fourier domain. It is well suited to image-processing applications because of its mathematical properties: a smooth and infinitely differentiable shape, the monomodal modulus and the optimal joint localization of space, orientation and frequency. Moreover, as a model, the 2D Gabor function closely mimics the properties of simple receptive fields in the primary visual cortex (V1) of primates in the statistics of natural images [18].

The use of filters with transfer functions that are Gaussian when viewed on the logarithmic frequency scale results in superior encoded natural images [19]. In particular, log-Gabor filters better discriminate the image features than Gabor filters. This result can be attributed to the transfer function, which is viewed at a logarithmic frequency scale that includes the limitation of maximum bandwidth; this scale is confined to approximately one octave on Gabor filters. However, this value is below the desirable value to achieve broad spectral information and maximum spatial localization.

Among several texture-orientated methods for palmprint recognition, LBP is an outstanding and effective descriptor of texture features. It is resistant to changes in rotation and illumination. The experimental method in this paper

combines the LBP descriptor with spiral feature extraction, which results in a daughter descriptor with a recognition performance that exceeds the parent descriptor.

### 3 Our contribution

The main contributions of this work are as follows:

- A new method based on feature selection from the fusion feature of LBP and spiral features for palmprint recognition.
- Extensive experiments are performed on three different palmprint databases (PPDBs): the PolyU palmprint database (PPDB) [12] with 356 subjects, the IIT Delhi contactless PPDB with 236 subjects [23] and the multi-spectral PolyU PPDB [20] with 500 subjects.
- Comprehensive analysis by comparing the proposed scheme with different state-of-the-art contemporary schemes based on the binarized statistical image features (BSIF) [21], Gabor transform [5], palm-code [6], fusion-code [11], double-orientation code [8] and oriented multiscale log-Gabor filters [22].

## 4 Proposed method

The proposed method pipeline for palmprint recognition (PPR) based on LBP and spiral features is shown in Fig. 1. The scheme comprises two steps.

### 4.1 Region of interest extraction

The key point identification method in [23] was used to determine the key points, which were used to align the palmprint image. With the aligned palmprint image, an region of interest (ROI) measuring  $128 \times 128$  was extracted. A sample

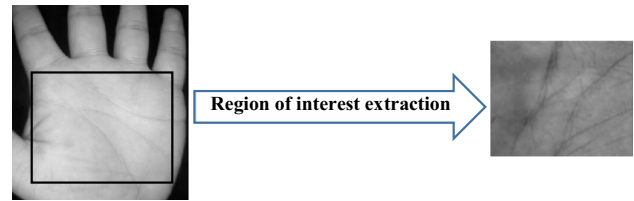


Fig. 2 Region of interest extraction

palmprint and the extracted ROI are shown in Fig. 2. The ROI extraction was only performed on samples from the PolyU PPDB because images were available in the MSPolyU and IITD databases.

### 4.2 Feature extraction

#### 4.2.1 Local binary pattern (LBP)

This section describes the traditional feature extraction method founded on block selection modes, as described in [24].

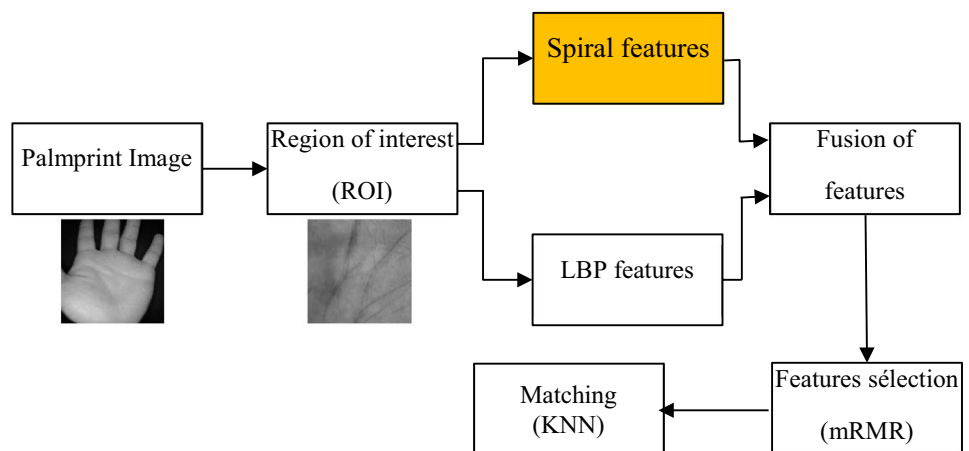
The binary code is the corresponding feature value and multiscale texture analysis with changing  $P$  and  $R$  values. The formula description is as follows:

$$\text{LBP}_{P,R} = \sum_{p=0}^{P-1} s(g_p - g_c)2^p, \quad s(x) = \begin{cases} 1 & x \geq 0 \\ 0 & x < 0 \end{cases}, \quad (1)$$

where  $g_c$  is the gray value of the center pixel,  $P$  is the neighbors and  $R$  is the sampling radius.

To be consistent with the traditional texture feature extraction method, a uniform LBP descriptor is used [25] to obtain palmprint images, which are divided into blocks with  $m \times n$  structure. Feature vectors are extracted for each block using the following formula:

Fig. 1 Proposed method pipeline



$$h = \{h^1, h^2, \dots, h^n\}, \quad (2)$$

where  $h$  is the final extracted feature vector,  $h^n$  is the histogram for each block and  $n$  is the total number of blocks. For example, using the uniform LBP descriptor to extract the feature, there are 16 blocks ( $n=16$ ); each block  $h^n$  corresponds to a histogram with 16 bins (dimensional feature vector). Therefore, the final uniform feature vector  $h$  is a 256-dimensional feature vector ( $16 \times 16 = 256$ ) (see Figs. 3, 4).

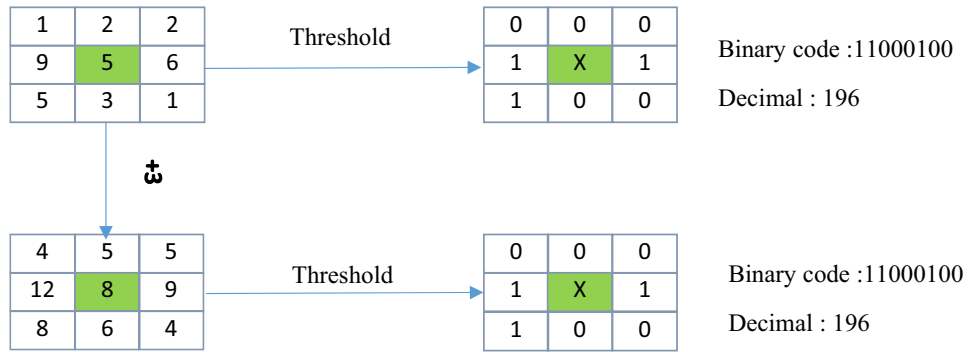
#### 4.2.2 Spiral of statistical local features (SSLF) (our approach)

##### 4.2.2.1 Statistical local features

- *Mean*: The mean is defined as

$$\text{mean} = \bar{X} = \frac{1}{n} \sum_{i=1}^n X_i \quad (3)$$

**Fig. 3** Diagram of the LBP descriptor and gray-scale invariant



- *Skewness*: This method measures the symmetry [26]. When the left and right sides of a central point are similar, the data set can be considered symmetrical. The skewness is defined as

$$\text{ske} = \frac{\frac{1}{n} \sum_{i=1}^n (X_i - \bar{X})^3}{\left[ \frac{1}{n} \sum_{i=1}^n (X_i - \bar{X})^2 \right]^{3/2}} \quad (4)$$

- *Kurtosis*: The kurtosis defines the sharpness of a peak relative to a normal distribution in a frequency distribution curve [26]:

$$\text{kurt} = \frac{\frac{1}{n} \sum_{i=1}^n (X_i - \bar{X})^4}{\left[ \frac{1}{n} \sum_{i=1}^n (X_i - \bar{X})^2 \right]^2} \quad (5)$$

##### 4.2.2.2 Spiral approach

Our approach is based on the moment features, ske (skewness) and kurt (kurtosis).

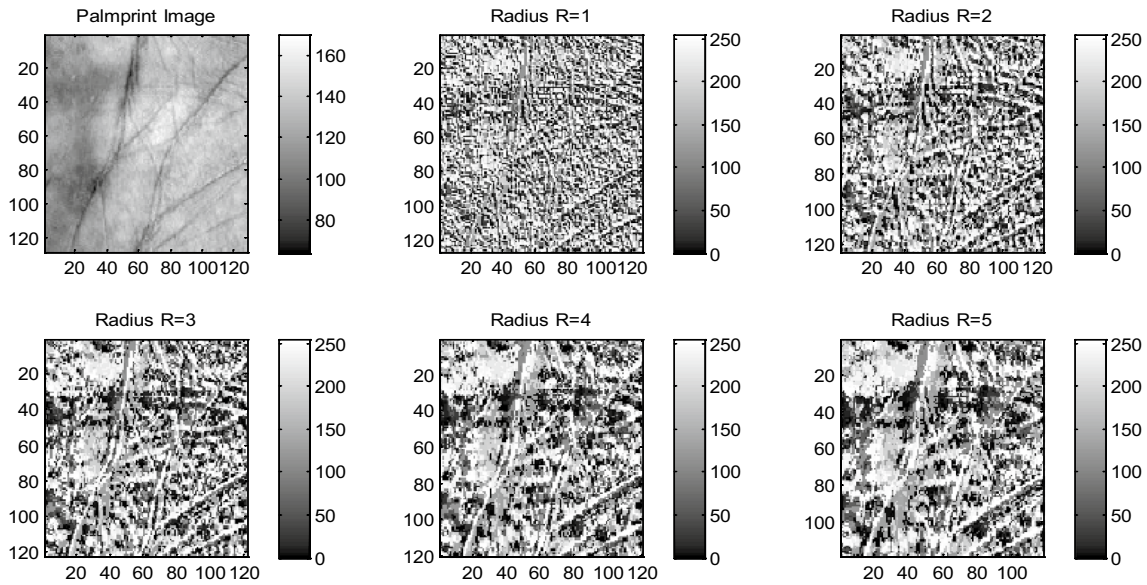


**Fig. 4** Samples from the MSPolyU database and the corresponding LBP codes

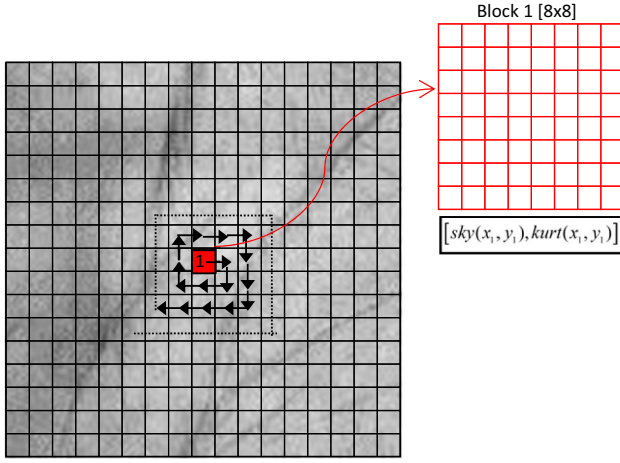


Fig. 5 Feature extraction scheme based on spiral feature extraction

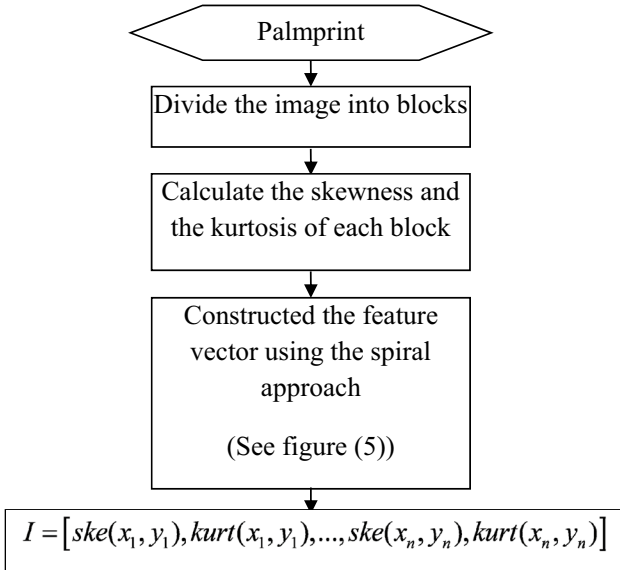


Fig. 6 Spiral algorithm flowchart

The image is divided into equally sized blocks ( $8 \times 8$ ). Starting at the central block, the process advances by one block at a time in a clockwise manner, as demonstrated in Figs. 5 and 6, the result is the feature vector  $I = [\text{ske}(x_1, y_1), \text{kurt}(x_1, y_1), \dots, \text{ske}(x_n, y_n), \text{kurt}(x_n, y_n)]$ , where  $n$  is the block's number.

### 4.3 Feature-level fusion

Feature-level fusion results in fuller biometric details because the biometric information is combined before being matched. Compared to the score-level fusion, feature-level fusion has a shorter response time. Creating a linked series of extracted features is the simplest type of feature-level

fusion, but concatenation may result in the “curse of dimensionality.” To offset the poor learning performance of the high-dimensional fused feature vector data, mRMR transformers are used.

#### 4.3.1 Normalization of the feature vector

Because of the variation in range and distribution, feature vectors that are independently extracted from LBP and spiral features are incompatible. To solve this issue, a normalization scheme (min–max, z-score, median) can be used to normalize the feature vectors. Here, the min–max normalization scheme is applied, which normalizes the feature vectors in the range  $[0, 1]$ . Let  $X = [x_1, x_2, x_3, \dots, x_n]$  be the feature vector, the normalized feature vector  $X'$  can be represented using min–max normalization (6).

$$X' = \frac{x_i - \text{Min}(X)}{\text{Max}(X) - \text{Min}(X)} \quad (6)$$

#### 4.3.2 Fusing the feature vector

By concatenating the normalized feature vectors of BSIF and spiral features into a single fused vector, the definitive fused vector is achieved. Let  $E_I = [e_1, e_2, e_3, \dots, e_n]$  and  $I_I = [i_1, i_2, i_3, \dots, i_n]$  be the normalized feature vectors of BSIF and spiral extraction, respectively. The fused vector is

$$\text{Fused}_{\text{vector}} = [e_1, e_2, e_3, \dots, e_n, i_1, i_2, i_3, \dots, i_n] \quad (7)$$

### 4.4 Feature selection based on mRMR

In this work, we determine the most appropriate subsets of features to model and yield a minimal error rate. The mRMR technique was selected to identify the prime features and palmprint recognition [27]. mRMR is commonly used as a feature selection method to select the most relevant features from subsets of features and the output class.

The input features in this experiment are fused features (LBP + spiral), from which the best features are selected and used to recognize the palmprint image, as shown in (8), where  $S$  is the subset of selected features, and  $\Omega$  is the pool of all input features. The minimum redundancy can be computed by

$$\min_{S \subset \Omega} \frac{1}{|S|^2} \sum_{i,j \in S} I(f_i, f_j), \quad (8)$$

where  $I(f_i, f_j)$  is the mutual information between  $f_i$  and  $f_j$ , then  $|S|$  is the number of input features of  $S$ . The mutual information  $I(C, f_j)$  is usually used to calculate the discrimination ability from feature  $f_i$  to class  $C = \{c_1, c_2, c_3, \dots, c_k\}$ . Therefore, the maximum relevancy is calculated by

$$\max_{S \subset \Omega} \frac{1}{|S|} \sum_{i \in S} I(C, f_j). \quad (9)$$

Combining (1) and (2), we obtain the following mRMR feature selection criterion in either the quotient form

$$\max_{S \subset \Omega} \left\{ \frac{\sum_{i \in S} I(C, f_j)}{\left[ \frac{1}{|S|} \sum_{i, j \in S} I(f_i, f_j) \right]} \right\} \quad (10)$$

or the difference form

$$\max_{S \subset \Omega} \left\{ \sum_{i \in S} I(C, f_j) - \left[ \frac{1}{|S|} \sum_{i, j \in S} I(f_i, f_j) \right] \right\} \quad (11)$$

In mRMR, features are incrementally added to the selected feature subset. The sequence of the incremental addition can be considered an “order of discrimination” ability of features. Thus, feature ordering can be calculated by (3) or (4) if all features have been entered into the selected subset by mRMR.

#### 4.5 *k*-Nearest-neighbor (KNN) classifier

To perform palmprint recognition using the KNN (*k*-nearest neighbors) scheme, the similarity criterion of a nearest-neighbor classifier is based on  $X^2$  [28].  $X^2$ , which is derived from the assumption that  $U = (\lambda_1, \lambda_2, \dots, \lambda_{10})$  and  $Q = (\rho_1, \rho_2, \dots, \rho_{10})$  are the feature vectors (i.e., histograms) extracted from the PPI and reference image, is computed as follows:

$$X^2 = \frac{1}{2} \sum_{i=1}^B \frac{(\lambda_i - \rho_i)^2}{(\lambda_i + \rho_i)} \quad (12)$$

If  $X^2 = 0$ , the histograms  $U$  and  $Q$  are comparable, but achieving a perfect match is unlikely in practice [28]. Therefore, a threshold  $T$  is introduced to compare the similarity measure  $X^2$  of the histograms. Then, the two feature vectors are from the same PPI if  $X^2 \leq T$ .

## 5 Experimental study

To test the validity of the scheme, exhaustive experiments were conducted using the available data in three large-scale, publicly available PPDBs: (1) PolyU PPDB [20], (2) IIT Delhi PPDB [23] and (3) multispectral PolyU PPDB [20]. The results are presented in terms of the equal error rate (EER) and recognition rates with their statistical validation.

### 5.1 PolyU palmprint database

This database contains the palmprints of 352 individuals, where 20 samples per individual were collected in two different sessions. All ten samples from the first session were

used as the control samples, and the second-session samples were the probe samples [12].

### 5.2 IIT Delhi palmprint database

For each of the 235 individuals who contributed to this database, there are five independently captured palmprint images per right and left palm. Four samples were selected for reference, and the remainder was used as the probe. This selection process was repeated using the leaving-one-out cross-validation with  $k=10$ . The results are the product of averaging the performance over all ten runs [23].

### 5.3 Multispectral PolyU palmprint database

This is the largest database with palmprints from 500 individuals. In each of two separate sessions, six samples per individual were captured in four different spectra: blue, green, red and near-infrared (NIR). The samples from the first session were denoted as reference samples; the second-session samples were the probe. The procedure was repeated for each spectral band, and the results are separately presented [20].

## 6 Results and discussion

### 6.1 Verification and identification rates

The combination of spiral features and LBP resulted in the last feature vector. To determine the accuracy of the technique, we applied different numbers of features of different sizes to palmprints from all three databases. The results are shown in Fig. 7. The histogram shows that  $R=5$  was the most accurate scheme. The most efficient number of features was 180.

The performance of the fused LPB and spiral with the mRMR method for the PolyU PPDB is presented in Table 1. Compared to other feature extraction methods (log-Gabor transform [5], palm-code [6], double-orientation code [8], fusion-code [11] and BSIF-SRC [21]), the experimental method has superior performance with an EER of 3.56%, which is a 1.5% improvement in EER.

The results demonstrate that for all three databases, the performance of the experimental method was equal to or better than that of six well-established PPR schemes. These findings validate the method, assure its robustness and reliability and make it suitable for palmprint recognition.

Table 2 presents the quantitative performances of various schemes on the IITD contactless PPDB. The data for the left and right palmprint samples are separately presented and show that the proposed scheme has the best performance

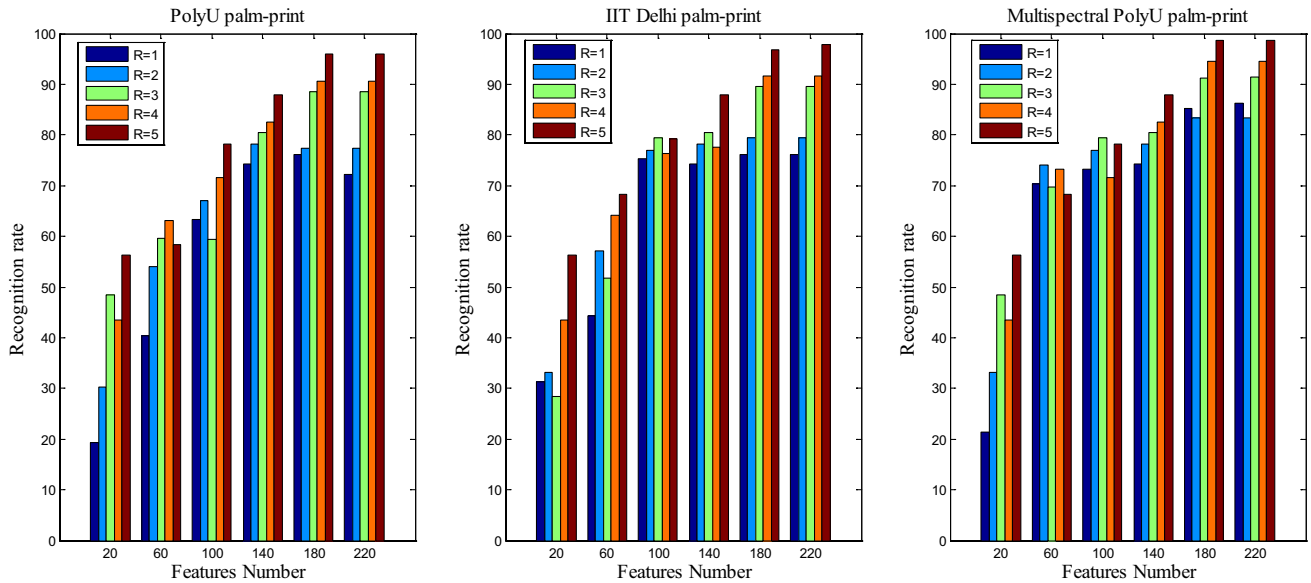


Fig. 7 Recognition rates of three databases (PolyU–IITD–MSPolyU)

Table 1 Performance of the proposed method on the PolyU palmprint database

Feature extraction	Matching technique	EER (%)
Proposed scheme (LBP + Spiral + mRMR)	Hamming distance	3.56
BSIF-SRC [21]	Sparse representation classifier	4.06
Double-orientation code [8]	Euclidean distance	9.2
Log-Gabor transform [5]	Hamming distance	7.96
Palm-code [6]	LDA classifier	14.66
Fusion-code [11]	Hamming distance	14.51

Table 2 Performance of the proposed method on the IIT Delhi palmprint database

IIT Delhi DB	Method	EER (%)	90% confidence interval
Left hand	Proposed scheme	0.07	[0.02; 0.12]
	BSIF-SRC [21]	0.42	[0.32; 0.52]
	Log-Gabor [5]	1.23	[0.93; 1.53]
	Palm-code [6]	2.67	[1.97; 9.37]
	Fusion-code [11]	2.34	[1.54; 3.14]
Right hand	Proposed scheme	0.32	[0.12; 0.52]
	BSIF-SRC [21]	1.31	[0.91; 1.71]
	Log-Gabor [5]	1.42	[1.02; 1.82]
	Palm-code [6]	3.41	[2.91; 3.91]
	Fusion-code [11]	3.39	[2.89; 3.89]

with an EER of 0.07 and 0.32% for the left and right palmprint samples, respectively.

The performance data for the multispectral PolyU PPDB are shown in Table 3. The performance of the proposed scheme matches that of BSIF-SRC [21] and log-Gabor [5] with an EER of 0% in each spectral band, which reaffirms the validity of the system.

## 6.2 Speed performance

The computation times of various algorithms in this work are listed in Table 4. All algorithms were developed in the MATLAB software and run on a PC with an Intel CORE i3 processor, 4 GB of RAM and Windows 7. All algorithms were implemented without speed optimization. Therefore, the computation times in Table 4 are only for reference.

## 7 Conclusion

In this paper, a new PPR approach is presented based on fusing spiral features and LBP filters and using mRMR to identify the best features. The feature extraction process begins with dividing the image into blocks; then, the skewness and kurtosis of each block are calculated before the feature vector is calculated using the spiral approach. The method was applied to palmprint images from three databases and was found to have a better identification and verification performance than the state-of-the-art methods.



**Table 3** Performance of the proposed method on the MSPolyU palmprint database

Spectrum	Method	EER (%) 90% confidence interval
Blue	Proposed scheme	0
	BSIF-SRC [21]	0
	Double-orientation code [8]	1.19
	Log-Gabor [5]	0
	Oriented multiscale log-Gabor filters [22]	[1.04–0.87]
	Palm-code [8]	0.2 [0.1; 0.3]
	Fusion-code [11]	0.4 [0.28; 0.68]
	LBP-SRC [29]	9.76 [8.36; 11.16]
	Green	Proposed scheme
BSIF-SRC [21]		0
Double-orientation code [8]		1.19
Log-Gabor [5]		0
Oriented multiscale log-Gabor filters [22]		[1.04–0.87]
Palm-code [6]		0.41 [0.21; 0.61]
Fusion-code [11]		0.67 [0.38; 0.96]
LBP-SRC [29]		17.75 [15.58; 19.92]
Red		Proposed scheme
	BSIF-SRC [21]	0
	Double-orientation code [8]	1.19
	Log-Gabor [5]	0
	Oriented multiscale log-Gabor filters [22]	[1.04–0.87]
	Palm-code [6]	0
	Fusion-code [11]	0.21 [0.03; 0.38]
	LBP-SRC [29]	14.78 [13.58; 15.98]
	NIR	Proposed scheme
BSIF-SRC [21]		0
Double-orientation code [8]		1.19
Log-Gabor [5]		0
Oriented multiscale log-Gabor filters [22]		[1.04–0.87]
Palm-code [6]		0
Fusion-code [11]		0.2 [0.02; 0.38]
LBP-SRC [29]		14.78 [13.38; 16.18]

**Table 4** Computation time of different algorithms in this work

Algorithms	Computation time in seconds
Proposed scheme	18
BSIF-SRC [25]	12
Log-Gabor [5]	25
Palm-code [6]	5
Fusion-code [11]	12
LBP-SRC [29]	10

**Acknowledgements** This work was conducted in the GREYC Laboratory in collaboration with the Algerian Ministry of Higher Education and Scientific Research. We thank our colleagues from the GREYC Laboratory in France who provided insight and expertise, thus greatly assisting the research.

## References

- Jain AK, Ross A, Nandakuma K (2011) Introduction to biometrics. Springer, Boston
- Zhang D, Guo Z, Lu Zhang L, Zuo W (2010) An online system of multispectral palmprint verification. *IEEE Trans Instrum Meas* 59:480–490
- Jia W, Huang D-S, Zhang D (2008) Palmprint verification based on robust line orientation code. *Pattern Recognit* 41:1504–1513
- Zhang D, Guo Z, Lu G, Zhang L, Liu Y, Zuo W (2011) Online joint palmprint and palmvein verification. *Expert Syst Appl* 38:2621–2631
- Tahmasebi A, Pourghasem H, Nasab HM (2011) A novel rank-level fusion for multi-spectral palmprint identification system. In: International conference on intelligent computation and biomedical instrumentation (ICBIMI), pp 208–211
- Zhang L, Li H, Niu J (2012) Fragile bits in palmprint recognition. *IEEE Signal Process Lett* 19:663–666
- Fei L, Xu Y, Zhang D (2016) Half-orientation extraction of palmprint features. *Pattern Recognit Lett* 69:35–41
- Fei L, Xu Y, Tang W, Zhang D (2016) Double-orientation code and nonlinear matching scheme for palmprint recognition. *Pattern Recognit* 49:89–101
- Badrinath GS, Gupta P (2008) Palmprint verification using SIFT features. In: First workshops on image processing theory, tools and applications (IPTA), pp 1–8
- Luo Y, Zhao L, Zhang B, Jia W, Xue F, Lu J, Zhu Y, Xu B (2016) Local line directional pattern for palmprint recognition. *Pattern Recognit* 50:26–44
- Ribaric S, Fratric I (2005) A biometric identification system based on eigenpalm and eigenfinger features. *IEEE Trans Pattern Anal Mach Intell* 27:1698–1709
- Zhang D, Kong W, You J, Wong M (2003) Online palmprint identification. *IEEE Trans Pattern Anal Mach Intell* 25:1041–1050
- Kumar A, Shen HC (2004) Palmprint identification using Palm-Codes. In: Third international conference on image and graphics (ICIG), pp 258–261
- Laadjel M, Bouridane A, Kurugollu F, Nibouche O, Yan WQ (2010) Partial palmprint matching using invariant local minutiae descriptors. In: Transactions on data hiding and multimedia security V, The series lecture notes in computer science, pp 1–17
- Laadjel M, Bouridane A, Nibouche O, Kurugollu F, Al-Maadeed S (2013) An improved palmprint recognition system using iris features. *J Real Time Image Process* 8:253–263
- Kong AW-K, Zhang D (2004) Competitive coding scheme for palmprint verification. In: The 17th international conference on pattern recognition (ICPR), pp 520–523
- Zuo W, Yue F, Wang K, Zhang D (2008) Multiscale competitive code for efficient palmprint recognition. In: The 19th international conference on pattern recognition (ICPR), pp 1–4
- Zuo W, Lin Z, Guo Z, Zhang D (2010) The multiscale competitive code via sparse representation for palmprint verification. In: IEEE conference on computer vision and pattern recognition (CVPR), pp 2265–2272
- Hong D, Liu W, Su J, Pan Z, Wang G (2015) A novel hierarchical approach for multispectral palmprint recognition. *Neurocomputing* 151:511–521

- 
20. Biometric Research Centre (UGC/CRC) at The Hong Kong Polytechnic University (2013) The Hong Kong Polytechnic University (PolyU) multispectral palmprint database. <http://www4.comp.polyu.edu.hk/~biometrics/MultispectralPalmprint/MSP.htm>. Accessed 13 Aug 2015
  21. Raghavendra R, Busch C (2015) Texture based features for robust palmprint recognition: a comparative study. *EURASIP J Inf Secur* 2015:1–9. <https://doi.org/10.1186/s13635-015-0022-z>
  22. Qian J, Yang J, Tai Y, Zheng H (2016) Exploring deep gradient information for biometric image feature representation. *Neurocomputing* 213:162–171
  23. Biometric Research Centre (UGC/CRC) at The Hong Kong Polytechnic University (2015) IIT Delhi Touchless Palmprint Database (Version 1.0). [http://www4.comp.polyu.edu.hk/~csajaykr/IITD/Database\\_Palm.htm](http://www4.comp.polyu.edu.hk/~csajaykr/IITD/Database_Palm.htm). Accessed 13 Aug 2015
  24. Kalluri HK, Prasad MVNK, Agarwal A (2012) Dynamic ROI extraction algorithm for Palmprints. In: Third international conference on advances in swarm intelligence (ICSI 2012), part II, pp 217–227
  25. Wang X, Gong H, Zhang H, Li B, Zhuang Z (2006) Palmprint identification using boosting local binary pattern. In: IEEE 18th international conference on pattern recognition, pp 503–506
  26. Ahonen T, Hadid A, Pietikäinen M (2006) Face description with local binary patterns: application to face recognition. *IEEE Trans Pattern Anal Mach Intell* 28:2037–2041
  27. Voigt K, Georgiou GM (2015) Stochastic computation of moments, mean, variance, skewness and kurtosis. *Electron Lett* 51:673–674
  28. Peng H, Long F, Ding C (2005) Feature selection based on mutual information: criteria of max-dependency, max-relevance, and min-redundancy. *IEEE Trans Pattern Anal Mach Intell* 27:1226–1238
  29. Dorsaf M, Boubchir L, Bouridane A, Nekhoul B, Ali-cherif A (2016) Multi spectral palmprint recognition-based-on-oriented-multiscale log Gabor filters. *Neurocomputing* 205:274–286